Remarks on $h \to aa \to 4b$ and $h \to aa \to 2\tau 2b$

Jack Gunion
U.C. Davis

Outline

1. **Models where this is relevant and relation to fine-tuning**

   Example, the NMSSM where fine-tuning is reduced (but not eliminated)

2. **The $2b2\tau$ final state, Ellwanger, Gunion, Hugonie Moretti**

3. **The Cheung, ... $4b$ study**

4. **The Carena Wagner, ... $4b$ study**

Models

- **NMSSM**

As you all know, in order to absolutely minimize EWSB fine-tuning in the context of SUSY, it is necessary to have $m_h \lesssim 100 \text{ GeV}$. This can escape LEP limits in the NMSSM via $h \rightarrow aa \rightarrow 4\tau$ decay.

However, the increase in the fine-tuning level is not huge if one requires $m_h > 110 \text{ GeV}$ (the LEP limit on the $4b$ channel) as allowed by LEP if $h \rightarrow aa \rightarrow 4b$ (with smaller rates for $2\tau 2b$ and 4τ).

However, $m_h > 115 \text{ GeV}$ starts to give much larger fine-tuning (unless large A_t, max-mix type scenarios are employed).

In addition, the "light-a-fine-tuning" measure G declines with increasing m_a (although I don't have the data needed to go beyond $m_a = 10$).

So, in some overall sense the total fine-tuning is remaining about the same in going from $m_h = 100 \text{ GeV}, m_a < 2m_\tau$ to $m_h = 110 \text{ GeV}, m_a > 2m_\tau$.

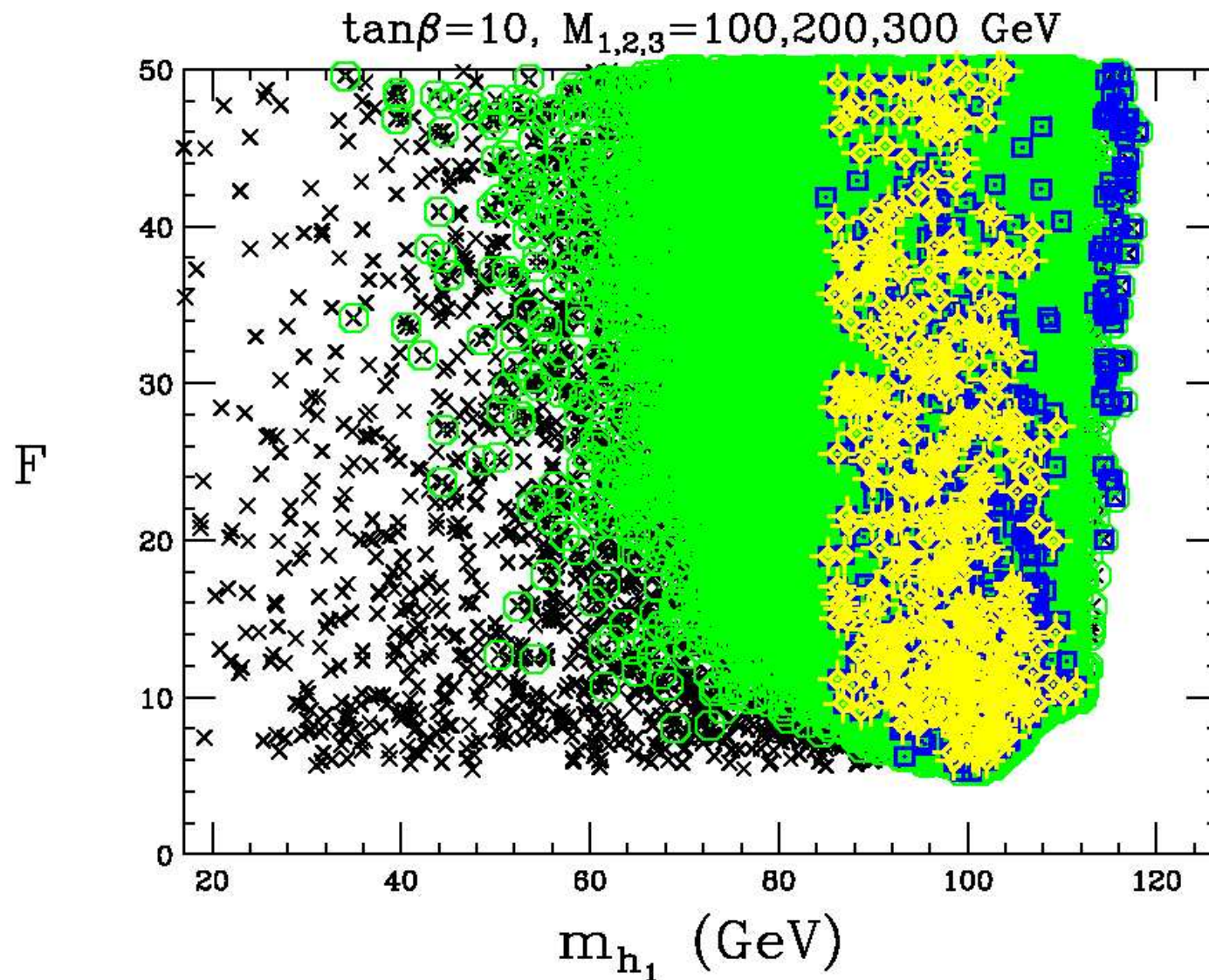**Unfortunately, the existing studies have focused on much larger m_a values than those for which we have examined G.**

Figure 1: The blue squares are the points that satisfy the LEP $Z + 4b$ final state limits, but not (until $m_h > 110$ GeV) the combined $Z + 2b$ and $Z + 4b$ LEP limits.

Main point: F increases from the lowest value of ~ 6 to $F \sim 10$ if $m_h > 110$ GeV is imposed. Not really so bad!
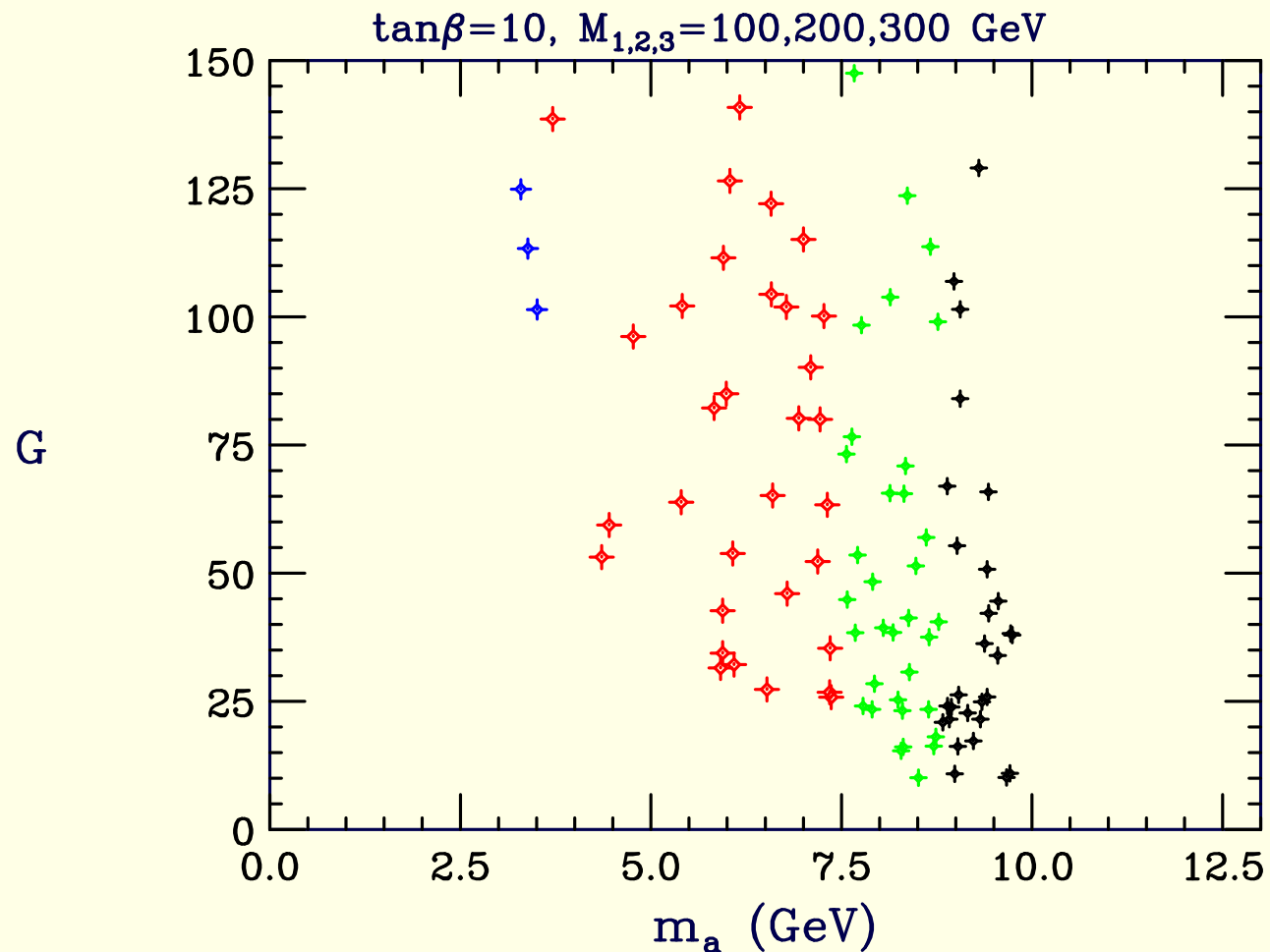
Figure 2: Only $F < 15$ points are shown.

Main point: G declines with increasing m_a, probably plateauing at about 10 or so for $m_a > 10$ GeV.

The LHC $WW \to h \to aa \to jj\tau^+\tau^-$ mode

- In earlier work, we (Ellwanger, Gunion, Hugonie, Moretti) studied 6 (different) points (four with $m_a \sim 30-50 \, \mathrm{GeV}$ and $m_h \sim 100-120 \, \mathrm{GeV}$) where this might be the only Higgs discovery mode at the LHC.

- After many cuts, including forward / backward jet tagging and various vetoes, but no b-tagging, we were able to eliminate the potentially serious DY $\tau^+\tau^- + jets$ background, leaving $t\bar{t}$ as the major background.

- We employed the usual ATLFAST tools and such and tried to include all kinds of reducible and irreducible backgrounds.

- We obtained the signals in the $M_{jj\tau^+\tau^-}$ distribution shown in Fig. 3.

  For all six cases, the Higgs resonance produces a bump at low $M_{jj\tau^+\tau^-}$ with lots of events (for $L = 300 \, \mathrm{fb}^{-1}$) and very high $S/\sqrt{B}$ values.

The main issue is whether or not the tail from the $t\bar{t}$ background really cuts off where shown.

Some ATLAS people (Zerwas, Baffioni) use different cuts and claim not, but they never really finished their study.
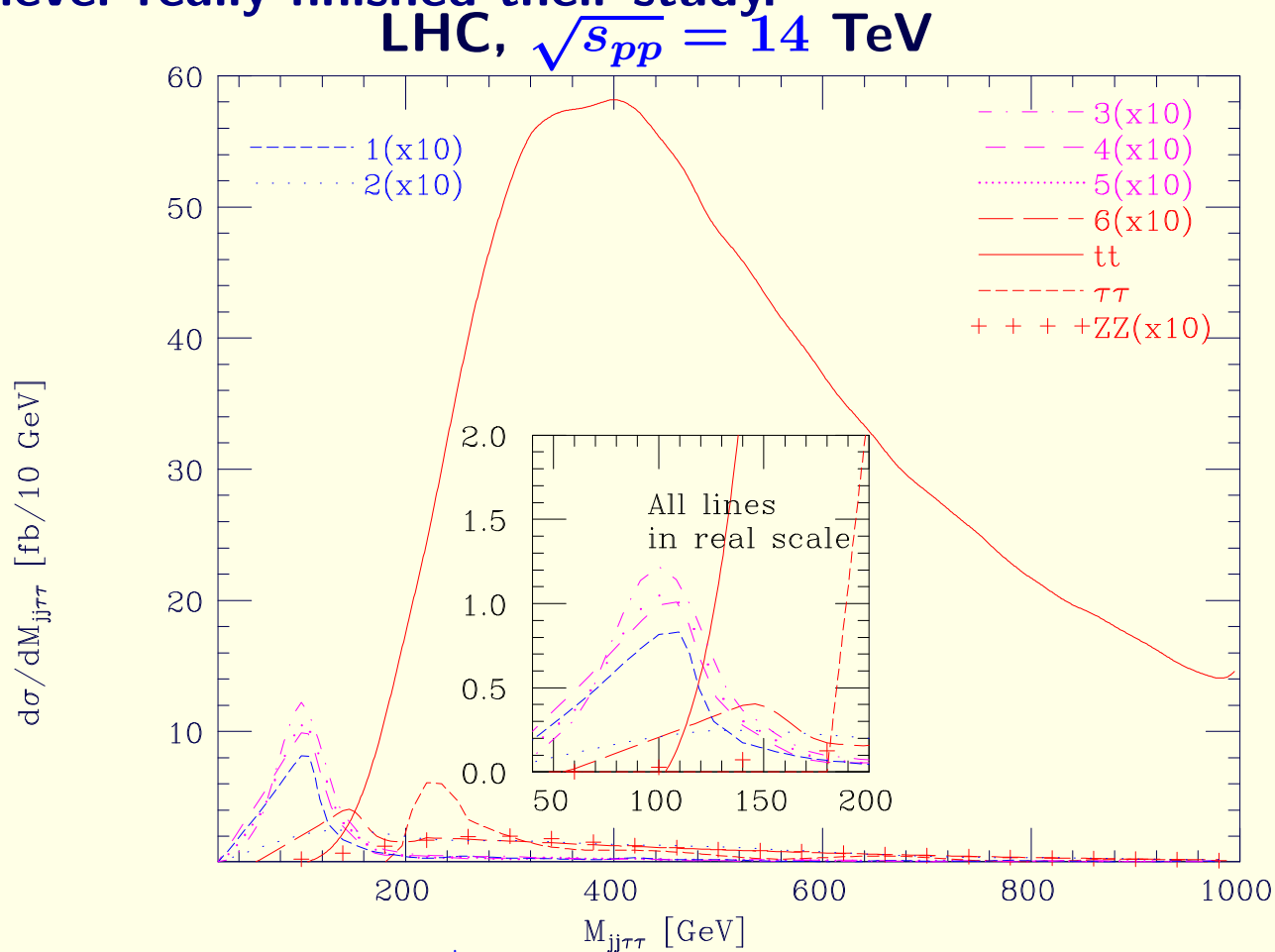

Figure 3: *Reconstructed mass of the $jj\tau^+\tau^-$ system for signals and backgrounds before b-tagging. No K factors are included.*

- **They focus on Wh and Zh production at the LHC, followed by the leptonic decay of the W and Z, and $h \to \eta\eta \to b\bar{b}b\bar{b}$.**

  In the final state, they require a charged lepton and four b-tagged jets. The advantage of having a charged lepton in the final state is to suppress the QCD background.

  The reason to require 4 b-tagged jets is to avoid the huge $t\bar{t}$ background. They are still left with some irreducible backgrounds from $W + nb$ and $Z + nb$ production with $n \geq 4$, $t\bar{t}b\bar{b}$ and $t\bar{t}t\bar{t}$ production ($t\bar{t}t\bar{t}$ is much smaller than $t\bar{t}b\bar{b}$ and is ignored.)

- **They study the feasibility of searching for the Higgs boson using $Wh, Zh \to \ell^\pm \, (\ell = e, \mu) \, + 4b + X$ at the LHC.**

  A naive signal analysis at the Tevatron led to a signal rate that is too small for realistic detection.

- At the LHC, they found a sufficiently large signal rate with a relatively small background for $m_h \lesssim 160$ GeV.

  Reconstructing the invariant mass of the 4 b-tagged jets is shown to play a crucial role:

  The signal will peak at m_h while the serious background begins at $M_{4b} \gtrsim 160$ GeV.

- They employ two NMSSM models and the SLHμ model.

- The dominant production for an intermediate Higgs boson at the LHC is gluon fusion. However, as mentioned above the decay $h \to \eta\eta$ followed by $\eta \to b\bar{b}$ is overwhelmed by QCD backgrounds.

  The next production mechanism, WW fusion, has the final state consisting of only hadronic jets.

  Therefore, they consider the associated production with a W or Z boson.

  The cross section is proportional to the square of the coupling g_{VVh}. In the NMSSM, the deviation of g_{VVh} from the SM value depends on the nature of the h_1.

For the bench-mark points #2 and #3 of Ellwanger, JFG, Hugonie, the size of g_{VVh} is very close to the SM value, though the sign may be opposite.

They consider 2 bench-mark points A and B, which are very similar to the earlier bench-mark points #2 and #3; these were found by scanning the parameter space using NMHDECAY.

They employed full helicity decays of the gauge bosons, $W \rightarrow \ell\nu$ or $Z \rightarrow \ell\ell$, and the phase decays of the Higgs boson and the pseudoscalar in $h \rightarrow \eta\eta \rightarrow b\bar{b}b\bar{b}$.

- **The detection requirements on the charged lepton and b jets in the final state are**

$$p_T(\ell) > 15\,\text{GeV}, \qquad |\eta(\ell)| < 2.5\,, \tag{1}$$
$$p_T(b) > 15\,\text{GeV}, \qquad |\eta(b)| < 2.5\,, \quad \Delta R(bb, b\ell) > 0.4\,,$$

where p_T denotes the transverse momentum, η denotes the pseudorapidity, and $\Delta R = \sqrt{(\Delta\eta)^2 + (\Delta\phi)^2}$ denotes the angular separation of the b-jets and the lepton. The smearing for the b jets is $\frac{\Delta E}{E} = \frac{0.5}{\sqrt{E}} \oplus 0.03\,$, where E is in GeV.

- In order to minimize the reducible backgrounds, they require at least one charged lepton and 4 b-tagged jets in the final state.

  They employ a B-tagging efficiency of 70% for each B tag ***which is very high and partly explains their better results compared to Carena etal***, and a probability of 5% for a light-quark jet faking a B tag.

  The backgrounds from $W + nj$ and $Z + nj$ contribute at a very low level and are reducible as they require 4 b-tagged jets in the final state.

  The background from $WZ \rightarrow \ell\nu b\bar{b}$ is also reducible by the 4 b-tagging requirement.

  So is QCD production of $t\bar{t}$ pair with one of the tops decaying hadronically and the other semi-leptonically.

  Jets from the W decay may fake a b-tag. This background is under control after applying the cuts.

  Note: no mention of $W2j2b$ reducible background, which is the dominant one for Carena et. al.

- While most of the backgrounds are reducible, there are a few channels that are irreducible.

They are (i) $t\bar{t}b\bar{b}$ production (**keep an eye on this one**), and (ii) $W/Z + 4b$ production.

- ### Results

In NMSSM, they chose two bench-mark points, A and B, both of which have $B(h \to a_1 a_1) \approx 1$ and $B(a_1 \to b\bar{b}) \approx 0.9$.

In a large portion of the parameter space of NMSSM, the mass of h_1 is around $100 \; \mathrm{GeV}$ and $B(h_1 \to a_1 a_1) \gtrsim 0.7$. The bench-mark points employed are quite common in the NMSSM.

In the **SLH**μ model, they employ two points in the parameter space such that the mass of the Higgs boson is $\mathcal{O}(100)$ **GeV** and $B(h \to \eta\eta) \gtrsim 0.7$.

The signal cross sections of Wh and Zh for the NMSSM and for **SLH**μ are shown in Table 1, and various backgrounds in Table 2, respectively.

(I can't understand cross section differences in NMSSM model B vs. model A yet. C_{4b}^2 is almost the same for the two models. The m_a value is higher for model B. Does the acceptance etc. increase so rapidly with m_a?)

Table 1: Signal cross sections for Wh and Zh production for bench-mark points NMSSM (A) and NMSSM (B), and for SLHμ (A) and SLHμ (B) at the LHC.

Channels	NMSSM (A)	NMSSM (B)	SLHμ (A)	SLHμ (B)
	$\lambda = 0.18$, $\kappa = -0.43$	$\lambda = 0.26$, $\kappa = 0.51$	$f = 4$ TeV	$f = 2$ TeV
	$\tan\beta = 29$	$\tan\beta = 23$	$\mu = 20$ GeV	$\mu = 20$ GeV
	$A_\lambda = -437$ GeV	$A_\lambda = -222$ GeV	$x_\lambda = 5.86$	$x_\lambda = 10$
	$A_\kappa = -4$ GeV	$A_\kappa = -13$ GeV	$\tan\beta = 17$	$\tan\beta = 9.47$
	$\mu_{\text{eff}} = -143$ GeV	$\mu_{\text{eff}} = 144$ GeV		
	$m_{h_1} = 110$ GeV	$m_{h_1} = 109$ GeV	$m_h = 146.2$ GeV	$m_h = 135.2$ Ge
	$m_{a_1} = 30$ GeV	$m_{a_1} = 39$ GeV	$m_\eta = 68.6$ GeV	$m_\eta = 47.9$ GeV
	$B(h_1 \to a_1 a_1) = 0.92$	$B(h_1 \to a_1 a_1) = 0.99$	$B(h \to \eta\eta) = 0.65$	$B(h \to \eta\eta) = $
	$B(a_1 \to b\bar{b}) = 0.93$	$B(a_1 \to b\bar{b}) = 0.92$	$B(\eta \to b\bar{b}) = 0.85$	$B(\eta \to b\bar{b}) = $
	$g_{VVh_1}/g_{VVh}^{\text{SM}} = 0.99$	$g_{VVh_1}/g_{VVh}^{\text{SM}} = -0.99$	$g_{VVh}/g_{VVh}^{\text{SM}} = 0.57$	$g_{VVh}/g_{VVh}^{\text{SM}}$
	$g_{tth_1}/g_{tth}^{\text{SM}} = 0.99$	$g_{tth_1}/g_{tth}^{\text{SM}} = -0.99$	$g_{tth}/g_{tth}^{\text{SM}} = 0.79$	$g_{tth}/g_{tth}^{\text{SM}} = 0.$
	$g_{tta_1}/g_{tth}^{\text{SM}} = -2.4 \times 10^{-3}$	$g_{tta_1}/g_{tth}^{\text{SM}} = -1.2 \times 10^{-2}$	$g_{tt\eta}/g_{tth}^{\text{SM}} = -0.89$	$g_{tt\eta}/g_{tth}^{\text{SM}} = -$
	$C_{4b}^2 = 0.80$	$C_{4b}^2 = 0.83$	$C_{4b}^2 = 0.16$	$C_{4b}^2 = 0.11$
W^+h signal	3.13 fb	9.54 fb	1.27 fb	0.63 fb
W^-h signal	2.35 fb	6.55 fb	0.87 fb	0.44 fb
Zh signal	1.05 fb	2.76 fb	0.36 fb	0.18 fb

Table 2: Background cross sections using the same cuts and efficiencies as in Table 1.

Channels	cross sections (fb)
$t\bar{t}$	172 (NMSSM & SLHμ)
$t\bar{t}b\bar{b}$	236 (NMSSM), 284 (SLHμ A), 429 (B)
$W + 4b$	3.80 (NMSSM), 4.16 (SLHμ A), 4.63 (B)
$Z + 4b$	3.85 (NMSSM & SLHμ)

The cross sections are those including the cuts listed in Eq. (1).

- **They imposed a b-tagging efficiency of 0.7 for each b jet and a mis-tag efficiency of 0.05 for a light-quark jet to fake a b jet (but they don't discuss "reducible" backgrounds?).**

  They require at least one charged lepton and 4 b-tagged jets.

- **The quantity C_{4b}^2 defined by**

$$C_{4b}^2 = \left(\frac{g_{VVh}}{g_{VVh}^{\text{SM}}}\right)^2 B(h \to \eta\eta)\, B^2(\eta \to b\bar{b}) \tag{2}$$

  and tabulated in the Table shows very clearly the importance of the channel $h \to \eta\eta \to b\bar{b}b\bar{b}$.

  For example, the two NMSSM bench-mark points have $C_{4b}^2 > 0.8$ while those for SLHμ only have $C_{4b}^2 \simeq 0.1$.

  This explains why the significance of the SLHμ signals is much smaller than that of the NMSSM signals, shown in Table 3.

  The LEP Collaboration made model-independent searches for the Higgs bosons in extended models.

They put limits on the quantity C_{4b}^2 using the channel $e^+e^- \to Zh \to ZAA \to Z + 4b$. The bench-mark points listed in the Tables are consistent with the existing limits.
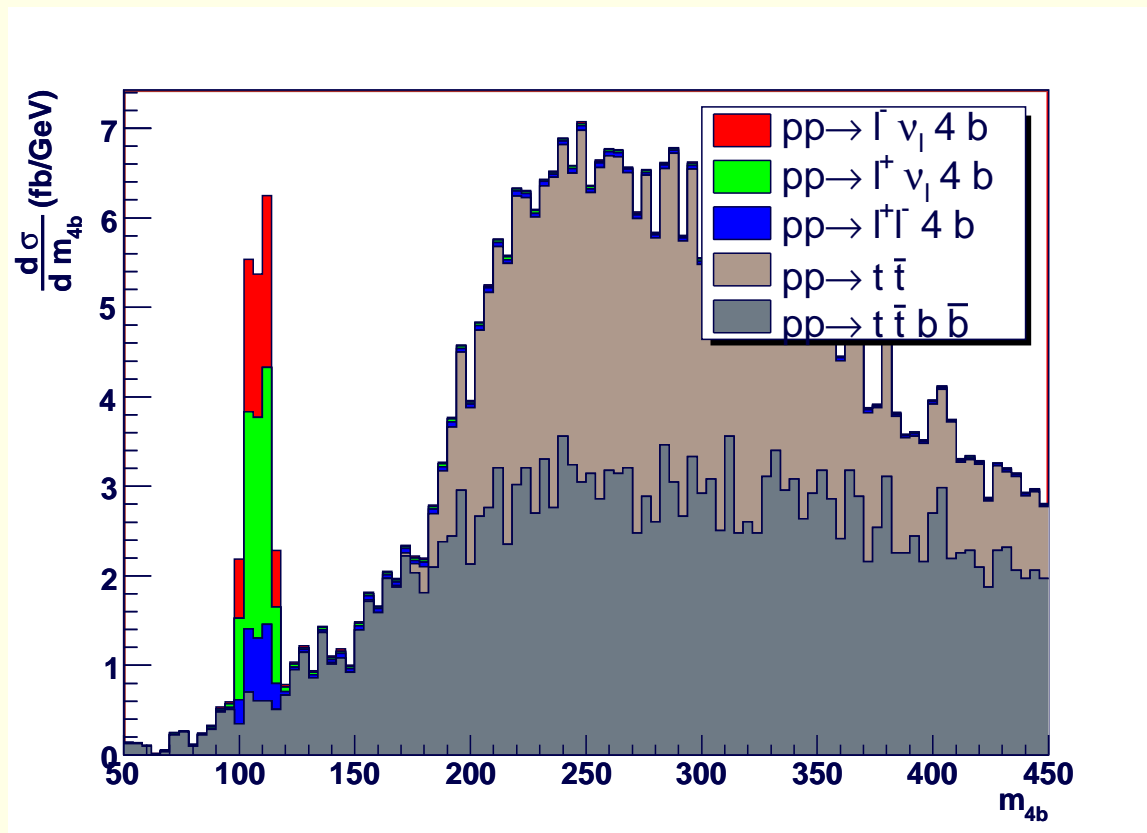

Figure 4: Invariant mass spectrum M_{4b} of the signal and various backgrounds for the bench-mark point B of the NMSSM.

- Since they require 4 b-tagged jets, they can easily reconstruct the invariant mass M_{4b} of the signal and the background.

  The invariant mass spectrum for the NMSSM point B is shown in Fig. 4.

  The spectra for other bench-mark points are similar.

  For $m_h \lesssim 160$ GeV the signal peak will stand out of the continuum, provided that the $B(h \rightarrow \eta\eta)$ still dominates.

  They calculate the significance of the signal by evaluating the signal and background cross sections under the signal peak:

  $$m_h - 15 \text{ GeV} < M_{4b} < m_h + 15 \text{ GeV} , \qquad (3)$$

  which is a conservative choice for the signal peak resolution.

  The total signal and background cross sections and the significance $S/\sqrt{B}$ appear in Table 3 using an integrated luminosity of 30 fb^{-1}.

  The significance of the NMSSM bench-mark points are large because of the smallness of background.

  On the contrary, the SLHμ bench-mark points have smaller significance but

close to 4 for point A, but not for point B. This is due to smaller signal rates and a much larger background from $t\bar{t}\eta$ production.

Table 3: Total signal and background cross sections after applying the cuts in Eq. (1) and the invariant mass cut of $m_h - 15 \text{ GeV} < M_{4b} < m_h + 15 \text{ GeV}$. The significance $S/\sqrt{B}$ is for a luminosity of 30 fb^{-1}.

	NMSSM		SLHμ	
	A	B	A	B
signal	6.53 fb	18.85 fb	2.50 fb	1.25 fb
bkgd	4.83 fb	4.77 fb	13.83 fb	22.45 fb
$S/\sqrt{B}$	16.3	47.3	3.7	1.4

- **Differences I have noticed compared to Carena et.al. in the next section.**

1. Cheung et. al. tag 4 b-jets but with a very high efficiency of 0.7. Carena et. al. claim $\epsilon_b \sim 0.5$ for $p_T > 15 \text{ GeV}$ b-jets and thus 4 b-tags cannot be afforded.
Note: $0.7^4 \sim 0.25$ vs. $0.5^3 \sim 0.125$
Even with fewer b tags, Carena et. al. signal cross sections are $5 - 10 \text{ fb}$ after cuts (at the LHC) compared to numbers like $6 - 18 \text{ fb}$ for Cheung et. al.

2. Cheung et. al. include the interesting $t\bar{t}b\bar{b}$ background which I don't believe was included in the Carena analysis.

   Cheung et. al. claim it is ultimately the dominant background, but then they have required 4 b-tags.

   However, even for 3 b-tags, it would seem that it should be put in if Cheung et. al. are right about the cross section.

3. A crucial question will be: Is $4b$ tagging sufficient to eliminate the $2b2j\ell\not{E}_T$ reducible background that as far as I can tell was not considered by Cheung et. al.?

4. $S/\sqrt{B}$ for Carena et. al. is much smaller as compared to Cheung et. al. Example:

   For Cheung et. al. model A, $S/\sqrt{B} \sim 16$ from $S \sim 6.53$ fb and $B \sim 4.83$ fb assuming $L = 30$ fb^{-1}.

   For Carena et. al. model with $C^2 \sim 0.5$, which yields similar S they get $S/\sqrt{B} \sim 5$ for $L = 30$ fb^{-1} mainly because of the much larger $B \sim 80$ fb from the reducible background of $2b2j\ell\not{E}_T$.

   And Carena et. al. will need to check the $t\bar{t}b\bar{b}$ background.

- **They concentrate on the $h \to aa \to 2b2\tau$ and $4b$ channels. The signal events being searched are**

$$Wh \to \quad l\nu_l, aa \quad \to \begin{cases} l\nu_l, b\bar{b}, b\bar{b} \\ l\nu_l, b\bar{b}, \tau^+\tau^- \end{cases} \tag{4}$$

$$Zh \to \quad l^+l^-, aa \quad \to \begin{cases} l^+l^-, b\bar{b}, b\bar{b} \\ l^+l^-, b\bar{b}, \tau^+\tau^-, \end{cases} \tag{5}$$

with $l = e, \mu$.

- **They define models of interest to be those for which**

$$\sigma(Vh) = \kappa_{hVV}^2 \sigma^{SM}(Vh). \tag{6}$$

lies in the range of $\kappa^2 \sim 0.5 - 1.0$, so that this Higgs contributes to the electroweak symmetry breaking. Consequently the associated production cross sections are sizable.

- **If the down quark and lepton coupling to the Higgs is proportional to their masses, then $BR(a \to b\bar{b})$ and $BR(a \to \tau^+\tau^-)$ are set to be 0.92 and 0.08, respectively.**

In general, however, the relations between the coupling and the masses may be modified by radiative corrections, which can lead to a large increase of the $BR(h \to \tau\tau)$.

The representative values and the ranges of the parameters are summarized in Table 4, all (they say) allowed by constraints from LEP, except for the region near $m_h \sim 90$ GeV if both a's are assumed to decay into two bottom quarks.

The overall factors modifying the SM results are

$$C^2_{2b2\tau} \equiv 2\kappa^2_{hVV} BR(h \to aa) BR(a \to b\bar{b}) BR(a \to \tau^+\tau^-), \qquad (7)$$

$$C^2_{4b} \equiv \kappa^2_{hVV} BR(h \to aa) BR(a \to b\bar{b})^2. \qquad (8)$$

	parameters	representative value	considered range
masses	m_h	120	$90-130$
	m_a	30	$20-60$
coupling	κ^2_{hVV}	0.7	$0.5-1.0$
branching fractions	$BR(h \rightarrow aa)$	0.85	$0.8-1.0$
	$BR(a \rightarrow b\bar{b})$	0.92	$0.95-0.50$
	$BR(a \rightarrow \tau^+\tau^-)$	0.08	$0.05-0.50$
$2b2\tau$ channel	$C^2_{2b2\tau}$	0.088	$0.038-0.50$
$4b$ channel	C^2_{4b}	0.50	$0.10-0.90$

Table 4: Parameter choices for $h \rightarrow aa$ decays. The C^2 factor is defined below.

- | The $2b2\tau$ channel at the Tevatron. |

Acceptance cuts at the Tevatron for the $2b2\tau$ channel:

$$p_T(l) > 15 \ \text{GeV}, \quad |\eta(l)| < 2.0, \quad \not{E}_T > 15 \ \text{GeV}. \tag{9}$$

Also, the taus and b's are tagged so as to suppress the SM backgrounds.

For the jets and other soft leptons in the events, the following basic cuts are employed to mimic the CDF detector acceptance. For jets

$$p_T(j) > 10 \ \text{GeV}, \quad |\eta(j)| < 3.0, \tag{10}$$

and for τ-candidates:

$$p_T > 10, 8, 5 \ \text{GeV for } \tau_h, \tau_e, \tau_\mu, \quad |\eta| < 1.5. \tag{11}$$

where τ_e, τ_μ and τ_h stand for the visible decay products of $\tau \rightarrow e\nu_e\nu_\tau$, $\tau \rightarrow \mu\nu_\mu\nu_\tau$, and $\tau \rightarrow \text{hadrons} + \nu_\tau$, respectively, and an isolation cut

$$\Delta R > 0.4 \tag{12}$$

between leptons, τ's and b-jets. After the acceptance cuts, $10 - 25\%$ of the signal events survive, and the cross section becomes $0.85 \ (0.57)$ fb for $m_h = 90 \ (130) \ \text{GeV}$ with the given set of input parameters ($C^2 \sim 0.088$). The cross sections passing acceptance are plotted in Fig. 5 versus the Higgs mass, represented by the circled curve. At this level, the cross section is below 1 fb.

The b- and hadronic τ-tagging efficiencies and the kinematics are taken to be

$$\epsilon_b = 50\% \quad \text{for } E_T^{jet} > 15 \text{ GeV} \quad \text{and } |\eta_{jet}| < 1.0 \ ,$$
$$\epsilon_\tau = 40\% \quad \text{for } E_{vis} > 20 \text{ GeV} \quad \text{and } |\eta| < 1.5 \ . \tag{13}$$

Outside these kinematical regions, the tagging efficiencies drop off sharply. We decide to tag one b and one tau. The energies for a jet and a lepton are smeared according a Gaussian distribution. The energy resolutions are taken to be

$$\frac{\Delta E_j}{E_j} = \frac{75\%}{\sqrt{E_j}} \oplus 5\%, \quad \frac{\Delta E_l}{E_l} = \frac{15\%}{\sqrt{E_l}} \oplus 1\%. \tag{14}$$

The missing energy is reconstructed according to the smeared observed particles. No further detector effects are included.

Irreducible Background

The dominant source of the irreducible background, with the same final state as the signal,

$$W \ Z^*/\gamma^*(\to \tau^+\tau^-) \ b\bar{b}, \tag{15}$$

has the $b\bar{b}$ pair from a virtual gluon splitting, the $\tau^+\tau^-$ pair from an intermediate Z^*/γ^* and the charged lepton plus missing energy from a W boson. Our simulations show that the largest contribution come from events with the Z^* almost on-shell, while the $\tau^+\tau^-$ pair from a virtual photon can be more easily confused with the signal. After applying the acceptance cuts, the irreducible background is estimated to be around 0.01 fb, which is very small compared to the signal size. It is essentially absent given the luminosity expected at the Tevatron.

Reducible Background

Reducible background arise from jets mis-identified as b's, or as hadronically decaying taus. The mistag rate per jet is taken to be around $0.5 - 1.0\%$ (0.5%) for tau (b).

In addition, the experiments cannot distinguish directly produced electrons (muons) from leptonically decaying taus.
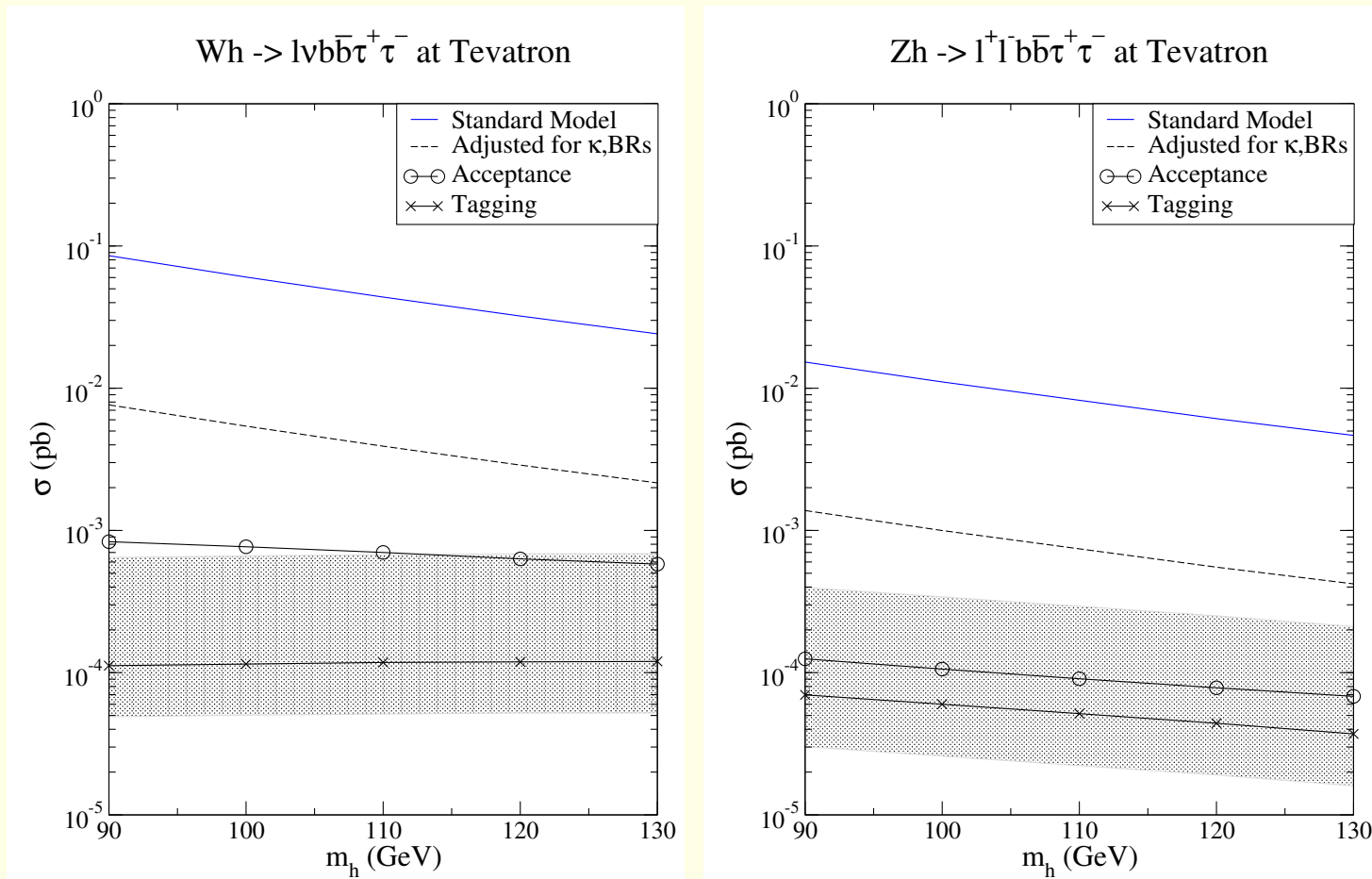
Figure 5: Cross sections of Higgs signal at the Tevatron in the $2b2\tau$ channel produced by Higgs-strahlung with a leptonically decaying W (left) or Z (right). Values of $m_a = 30$ GeV and $C^2 = 0.088$ are assumed, except for the shaded bands which correspond to variations of the value of C^2 within the range allowed by both our choice of parameters, Table 4, and the constraints from the LEP results.

The two bottom-quarks in the final state coming from the Higgs boson decays should have an invariant mass equal m_a.

If enough data were available, one would be able to observe an excess of events in the $m(2b)$ mass distribution. However, this procedure is heavily limited by statistics.

For instance, with a window cut of $m_a \pm 10$ GeV on $m(2b)$, the reducible background can be a factor of 3 to 5 smaller than the signal, but unfortunately, the cuts and the tagging efficiencies together reduce the signal greatly to about 0.11 fb for Wh and $0.05 - 0.07$ fb for Zh, with $C^2 \sim 0.088$ as shown in Fig. 5 by the crossed curve.

The shaded band represents the range of parameters allowed by our choice of $C^2 \sim 0.038 - 0.50$, consistent with the LEP constraints.

With an optimistic value of $C^2 \sim 0.50$, the cross section is 0.68 fb, and we would expect to see about a couple of signal events with an integrated luminosity of a few fb^{-1}.

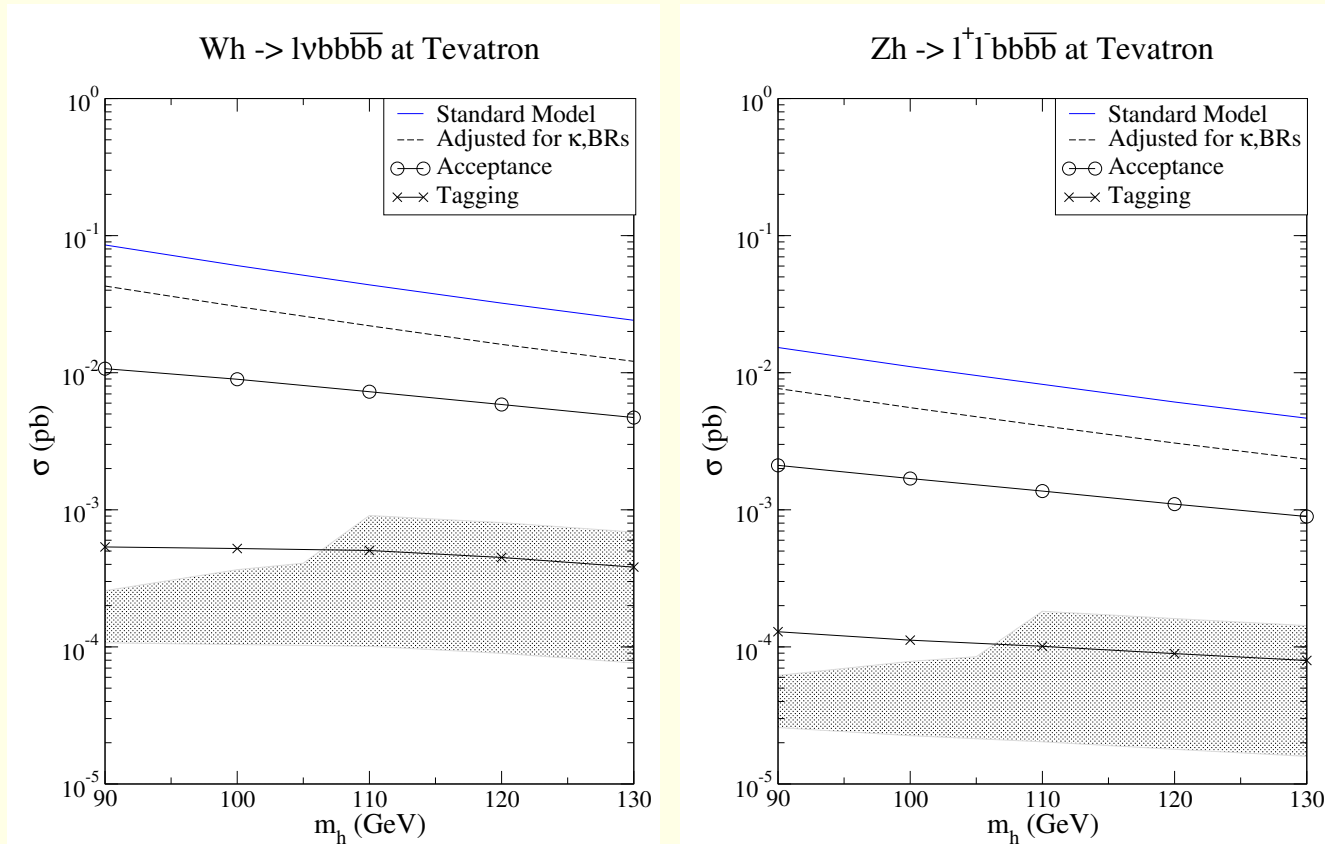- **The $4b$ channel at the Tevatron.**

Figure 6: Cross sections of Higgs signal at the Tevatron in the $4b$ channel produced by Higgs-strahlung with a leptonically decaying W (left) or Z (right). $m_a = 30$ GeV and $C^2 = 0.50$ are assumed, except for the shaded bands which correspond to vary C^2 within the values allowed by both our choice of parameters, Table 4, and constraints from the LEP results.

Similar to the $2b2\tau$ mode, the $4b$ cross section is

$$\sigma_{4b} = \sigma(Vh) \; BR(V) \; BR(h \to aa)BR(a \to b\bar{b})^2, \qquad (16)$$

from which we extract the C^2 factor

$$C_{4b}^2 \equiv \kappa_{hVV}^2 BR(h \to aa)BR(a \to b\bar{b})^2. \qquad (17)$$

The $4b$ mode is usually enhanced by the large branching fractions of the decay of a into bottom quarks. The ratio $C_{4b}^2/C_{2b2\tau}^2$ ranges in $9.5 - 0.5$ for $BR(a \to \tau\tau) \sim 0.05 - 0.50$. The value of C_{4b}^2 itself does not vary greatly with the branching fractions that are obtained within our choice of parameters, Table 4.

Despite larger background for this mode than for the $2b2\tau$ mode, the enhanced rate suggests this to be a more viable mode.

The parameter choices for the $4b$ channel are also given in Table. 4.

In parallel to the $2b2\tau$ channel, we plot the cross sections in Fig. 6.

The shaded bands show the LEP constraints disfavoring the lower end of the m_h range.

We find the signal rate after acceptance cuts to be $10.7 - 4.7$ fb (the circled curve) for $m_h = 90 - 130$ GeV with $C^2 \sim 0.5$.

After tagging three bottom jets (as needed to kill backgrounds) and imposing appropriate additional cuts, the cross section becomes $0.54 - 0.38$ fb (the crossed curve) for $m_h = 90 - 130$ GeV.

We again adopt the basic acceptance cuts and the b-tagging requirements as in the previous section.

The background for this mode arises from $4bl\not{E}_T$, $3bjl\not{E}_T$, $2b2jl\not{E}_T$, $b3jl\not{E}_T$ and $4jl\not{E}_T$ events.

For the four b's in our signal, tagging two will not be sufficient, as background from $2b2jl\not{E}_T$ events can fake the signal without any mistagging involved. Therefore we demand that at least three bottom jets be tagged.

The irreducible background $4bl\not{E}_T$, though much larger than that in the $2b2\tau$ mode, is still manageable. We find the cross section to be 0.23 fb after basic acceptance cuts. Like the signal events, it suffers similar reductions from tagging and further cuts, which brings it down to 0.02 fb. With tagging for $3b$'s, the $3bjl\not{E}_T$ events cannot be effectively distinguished from the signal either. They contribute about 0.003 fb to the background.

The reducible backgrounds from $2b2jl\not{E}_T$ and $4jl\not{E}_T$ events have the same sources as that in the $2b2\tau$ mode and the mistag rates of $jet \to b$ and $jet \to \tau$ are comparable. The tagging on the 3rd b brings this background down significantly. In total, they contribute about 0.07 fb to the background. $3bjl\not{E}_T$ and $b3jl\not{E}_T$ backgrounds combine for less than 0.003 fb.

Having tagged three of the four bottom quarks, we identify the fourth bottom as the hardest untagged jet in the event. We expect the signal to appear as a peak in the invariant mass $m(b_1, b_2)$ and $m(b_3, b_4)$ distribution. However, pairing the four b jets can be complicated due to combinatorics. We assign the two pairs by minimizing their mass difference $m(b_1, b_2) \approx m(b_3, b_4)$ and record both values each with a half weight.

We present the signal versus the background distributions of the reconstructed masses m_h and m_a in Fig. **7** as the invariant masses of four b-jets and of two b-jets. With a simple cut on the $m(4b)$ invariant mass, $m(4b) < 160$ GeV, dictated by our search for a light Higgs boson with mass smaller than about 130 GeV, the overall signal to background ratio can be about 10 with $C^2 = 0.50$, $m_a = 30$ GeV and $m_h = 90 - 130$ GeV.
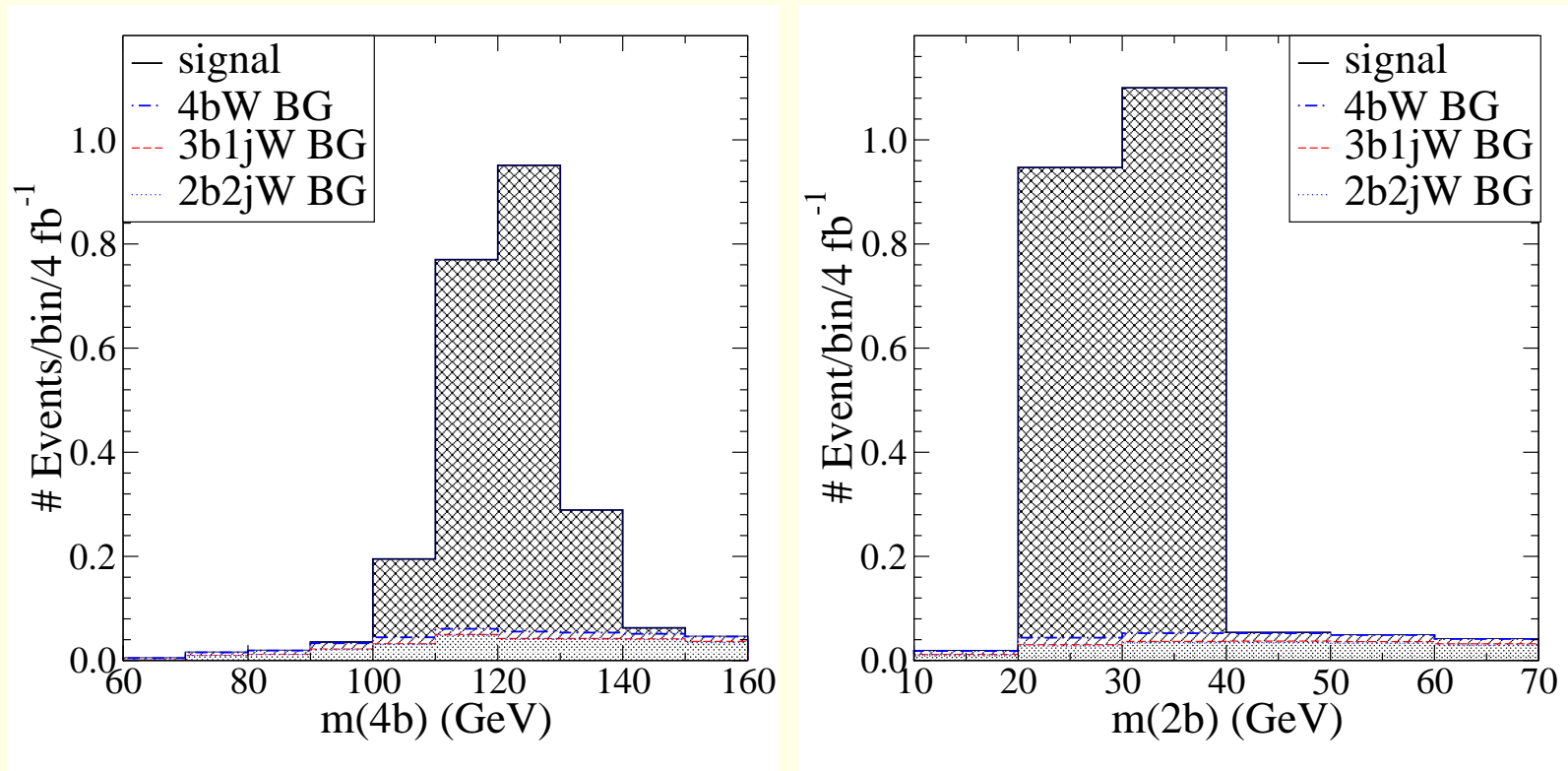
Figure 7: Higgs signal versus background at the Tevatron in the $4b$ decay channel together with a leptonically decaying W. The invariant mass of four (left) and two (right) b-jets are shown. Values of $C_{4b}^2 = 0.50$, $m_h = 120$ GeV and $m_a = 30$ GeV are understood.

To summarize the study at the Tevatron, they claim that the signal channels of Eqs. (4) and (5) have distinctive kinematical features (see Fig. 7) with negligible SM backgrounds and the signal observation is statistically dominated.

For the $2b2\tau$ mode, one can reach a cross section of about $0.05 - 0.7$ fb as shown in Fig. 5, while for the $4b$ mode, we have the cross section in the range of $0.1 - 1$ fb as shown in Fig. 6.

- $\boxed{h \to aa \text{ at the LHC}}$

At the LHC, weak boson-associated Higgs production rate is about $10 - 15$ times that at the Tevatron in the mass region we are interested in.

The (QCD) background, on the other hand, can be 100 times larger than at the Tevatron. This requires a substantial jet rejection rate. These cross sections are plotted in Fig. 8.

Cuts on the triggering leptons and/or missing energy are taken to be

$$p_T(l) > 20 \text{ GeV}, \quad |\eta(l)| < 2.5, \quad \not{E}_T > 20 \text{ GeV}. \tag{18}$$

The following cuts and efficiencies for tagging are assumed

$$\epsilon_b = 50\% \quad \text{for } E_T^{jet} > 15 \text{ GeV} \quad \text{and } |\eta_{jet}| < 2.0 \;,$$

$$\epsilon_\tau = 40\% \quad \text{for } E_{vis} > 15 \text{ GeV} \quad \text{and } |\eta| < 2.5 \;. \tag{19}$$

The jet rejection rate is better than 1/150 for tagging a b or a τ, except in the $15 - 30$ GeV p_T range where it is taken to be $\sim 1/30$, as there exists strong tension between tagging efficiencies and the jet rejection rates, especially near the low p_T range.

Note that the jet rejection rate will only be accurately known after understanding the detectors with examining the real data.

Again, in our simulations, the energies for a jet and a lepton are smeared with the Gaussian resolutions

$$\frac{\Delta E_j}{E_j} = \frac{50\%}{\sqrt{E_j}} \oplus 3\%, \quad \frac{\Delta E_l}{E_l} = \frac{10\%}{\sqrt{E_l}} \oplus 0.7\% \;. \tag{20}$$

The missing energy is reconstructed accordingly.

- ### The $2b2\tau$ Channel

Similar to the Tevatron case, the irreducible background of Eq. (**15**) is small after the acceptance cuts and the tagging requirements, contributing only 0.07 fb. The reducible background, however, poses a much more severe problem at the LHC. For example, the $2b2jl\not{E}_T$ events are estimated to be around 11 pb, compared to 50 fb at the Tevatron. Thus for the $2b2\tau$ mode, a jet rejection rate of 1/150 would give rise to a background of 92 fb, compared to the signal size about 1 fb (or up to $\sim$7 fb when maximizing C^2). The $4jl\not{E}_T$ events also contribute 43 fb to the background in this channel.

We carry out the analysis similar to the Tevatron case and arrive at a S/B ratio of 0.03, with a total signal size of less than 1 fb for $m_h = 120$ GeV, $m_a = 30$ GeV and $C^2 = 0.088$. The small S/B ratio would require precise control of the systematic errors. It can be further improved by tagging one more b or τ, at the expense of losing up to half of the signal rate.

Due to the difficulty of finding a signal in this channel, we are led to consider the more promising channel of $4b$'s, where, as we did in the Tevatron case, we employ an additional tagging, while still retaining a higher signal rate.
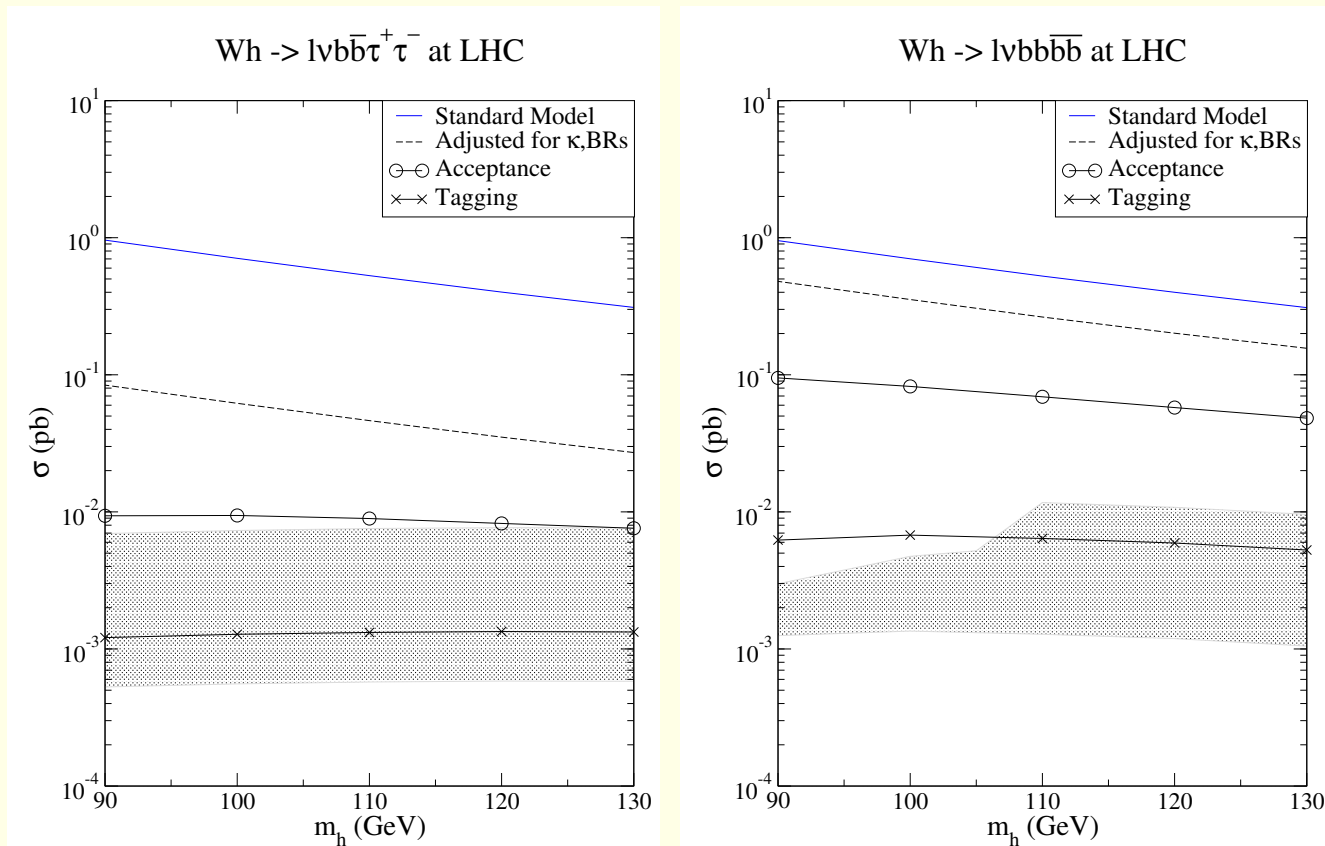
Figure 8: Cross sections of Higgs signal at the LHC in the $2b2\tau$ (left) and $4b$ (right) channels produced by Higgs-strahlung with a leptonically decaying W. $m_a = 30$ GeV, $C^2_{2b2\tau} = 0.088$ and $C^2_{4b} = 0.50$ are assumed, except for the shaded bands which correspond to variations of C^2 within the regions allowed by both our parameter choice, Table 4, and constraints from the LEP results.

- **The $4b$ Channel**

With a much higher luminosity than the Tevatron and larger cross sections, LHC could produce 60 ($10\,\mathrm{fb}^{-1}$) to over a thousand ($300\,\mathrm{fb}^{-1}$) Higgs events in the $4bl\not{E}_T$ decay channel, assuming a typical C^2 value ($C^2_{4b} = 0.50$), as shown in Fig. **8**.

The $4b$ channel is thus more optimistic for observing the Higgs, even though the background still dominates the signal, and the irreducible $4bl\not{E}_T$ background becomes non-negligible.

We require tagging three of the b jets, which would essentially eliminates backgrounds from $4jl\not{E}_T$, and reduces the $2b2jl\not{E}_T$ and $1b3jl\not{E}_T$ background significantly.

With three tagged b-jets, the signal rate is about $5.7\,\mathrm{fb}$ (or up to $10\,\mathrm{fb}$ when maximizing C^2).

The irreducible background $4bl\not{E}_T$ is $25\,\mathrm{fb}$. The $3bjl\not{E}_T$ background is about $16\,\mathrm{fb}$.

The reducible background from $2b2jl\not{E}_T$ events is about $80\,\mathrm{fb}$.

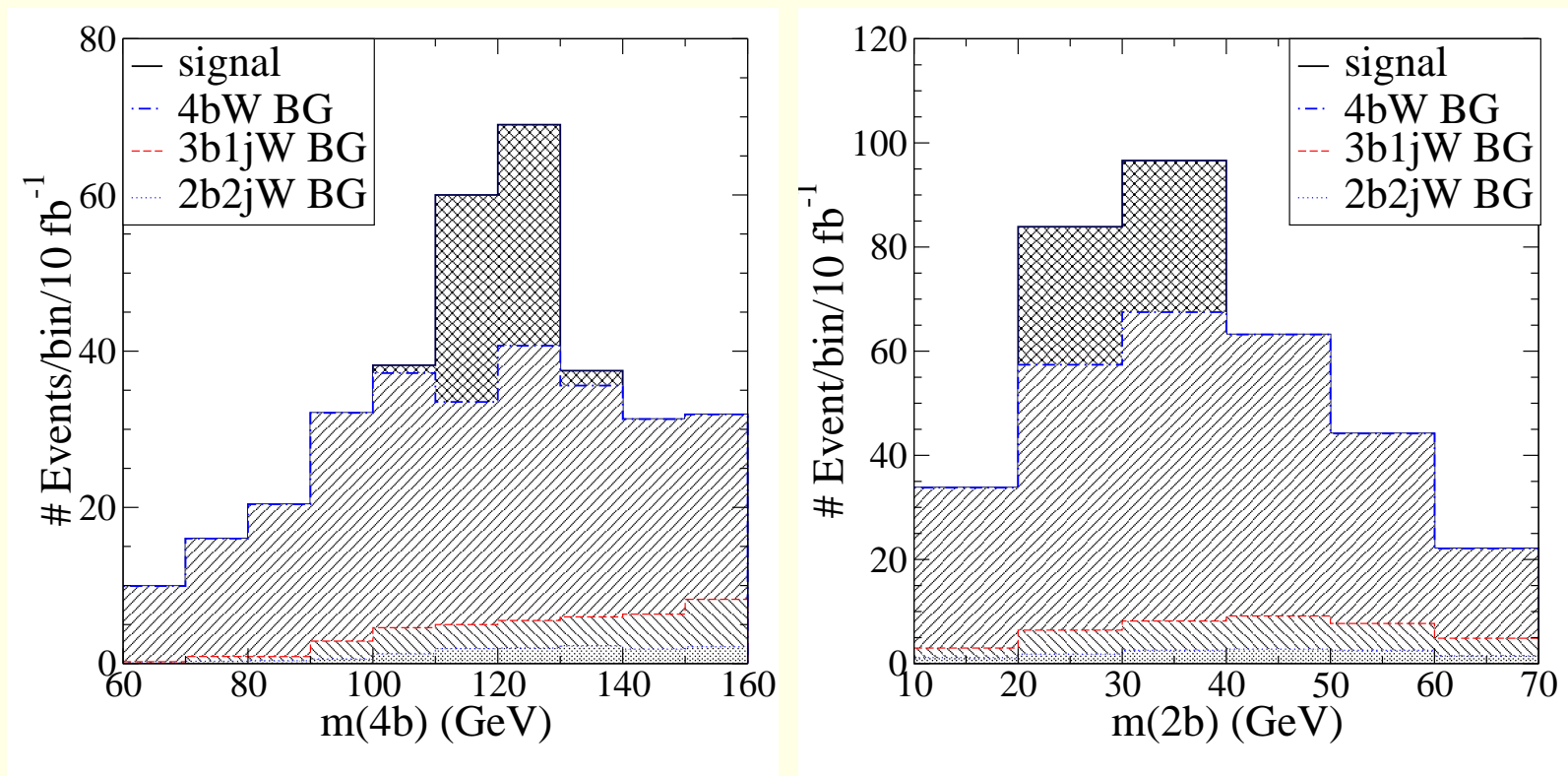# The $4jl\not{E}_T$ background is no larger than 0.2 fb.

Figure 9: Higgs signal versus background at the LHC in the $4b$ decay channel together with a leptonically decaying W. The invariant mass of four (left) and two (right) b-jets are shown. Constraints of 60 GeV $< m(4b) < 160$ GeV and 10 GeV $< m(2b) < 70$ GeV are implemented in both plots. $C_{4b}^2 = 0.50$, $m_h = 120$ GeV and $m_a = 30$ GeV are understood.

We again present the reconstructed mass distribution for the signal and backgrounds in two plots in Fig. **9**.

The left and right plots show the invariant mass distributions of the $4b$ and $2b$ system, where the signal peaks near $m_h = 120$ GeV and $m_a = 30$ GeV, respectively, each with a width less than 10 GeV due to detector energy resolution.

Similar to the Tevatron case, we assign the two bb pairs by minimizing their mass difference $m(b_1, b_2) \approx m(b_3, b_4)$ and plot these two masses, each with a half weight.

The dominant $2b2jlE_T$ background comes from $t\bar{t}$ production. For $t\bar{t}$ events, the $2b2j$ system contains all the decay products of a top-quark. Therefore, these events may be efficiently rejected with an upper cut on the $m(4b)$ invariant mass lower than the top quark mass, $m(4b) \lesssim 160$ GeV, which will not affect the signal we consider if the Higgs boson mass is in the region $m \lesssim 130$ GeV.

Given our considered range of choices, we implement the following constraints in the two distributions:

$$10 \text{ GeV} < \quad m(2b) \quad < 70 \text{ GeV} \,,$$

$$60 \text{ GeV} < \quad m(4b) \quad < 160 \text{ GeV}.$$

While the former affects the $m(4b)$ distribution minimally, the latter reduces the background in $m(2b)$ distribution by about 40%.

Overall, selecting events with these invariant mass constraints, the value of S/B is roughly $1/5$ for $C_{4b}^2 = 0.50$.

Assuming a good understanding of the background, one can get an estimate of the statistical significance of the signal.

For the rate quoted above we obtain a significance, $S/\sqrt{B}$, of over 3.5σ for 10 fb^{-1} and over 5σ for 30 fb^{-1}, as indicated in Fig. 9.

If one selects events only in the expected signal region, we obtain a $S/B \simeq 0.41$ in the range $100 \text{ GeV} < m(4b) < 140 \text{ GeV}$ from the $m(4b)$ distribution, and a $S/B \simeq 0.40$ in the range $20 \text{ GeV} < m(2b) < 40 \text{ GeV}$ from the $m(2b)$ distribution, equivalent to a reduction by about a factor of two of the luminosity necessary to achieve the same statistical significances.

The challenge is for us to understand the background well enough, and to control the systematic errors.

It may be a challenge at the LHC to retain the high b-tagging efficiency at $p_T \sim 15 \text{ GeV}$ adopted in the current analysis.

If a 30 GeV cut on the tagged jets is implemented instead, the signal is reduced to 22%, while the background drops to about 37% of the values given above.

In such case a 3σ (5σ) signal would require an integrated luminosity of around $30\,(80)$ fb^{-1}.

Therefore a good understanding of b-tagging efficiencies at low p_T will be necessary to be able to discover a Higgs in the $4b$ channels in the first years of the LHC.

- **Summary**

We analyzed the Wh channel in the mass range $90 \leq m_h \leq 130$ GeV in detail. We found that at the Tevatron

  – With only basic cuts, the signal size is 0.7 fb for the $2b2\tau$ channel for $C^2_{2b2\tau} \sim 0.088$ with a negligible irreducible background, and $5-10$ fb the $4b$ channel for $C^2_{4b} \sim 0.50$ with a comparable background. With favorable couplings and branching fractions, the C^2 factor can be as large as 0.50 for the $2b2\tau$ mode, and 0.90 for $4b$, and the signal rate is enhanced proportionally.

- Further cuts and the tagging of b and τ, necessary to remove the much larger reducible background, worsen the signal event rate to around 0.11 fb for the $2b2\tau$ mode and 0.5 fb for the $4b$ mode, as summarized in Figs. 5 and 6.

  However, the kinematics of the mass reconstruction of m_a and m_h can be very distinctive, as seen in Fig. 7 for the $4b$ mode with small background and a couple of total events.
- There can be another improvement of $15 - 30\%$ by combining Wh events with the Zh events, where both $Z \to ll$ and $Z \to \nu\nu$ can be included, leading to a possible observation of a few events in either $2b2\tau$ or $4b$ channel, for a Tevatron luminosity of the order of a few fb^{-1}.

Overall, the signal observation becomes statistically limited. Our study has been based on parameters of the CDF detector.

One expects the signal observability to be enhanced accordingly if results from the D0 detector were combined.

At the LHC, the signal rate increases by a factor of 10, and the background increases by two orders of magnitude, compared to the Tevatron. We found that

- Statistics limitation is no longer a major issue. In the $4b$ channel alone

the signal rate is 5.7 fb , and we can easily obtain a signal significance $S/\sqrt{B} > 3.5$ with an integrated luminosity of 10 fb^{-1}, and $S/\sqrt{B} > 10$ with 100 fb^{-1}.

– Similar to the Tevatron study, with favorable couplings and branching fractions, the signal rate can be enhanced to be as large as 10 fb with $C^2 = 0.9$, as seen in Fig. 8, and S/B can be improved accordingly.

– The kinematics of the mass reconstruction of m_a and m_h can be very distinctive, as seen in Fig. 9 for the $4b$ mode, yielding a statistically significant signal.

The main challenge would be to retain the adequate tagging efficiency of b's and τ's in the low p_T region.

We point out that our background analysis is based on the leading order partonic calculations in MadEvent. More accurate estimate of the background distributions would be important to claim a signal observation.

More realistic simulations including the detector effects are needed to draw more convincing conclusions.